On the Apparent Fluorescence Recovery Due to Electrosorption

Jeff L. Shepherd and Dan Bizzotto*

Department of Chemistry, University of British Columbia, Vancouver, 2036 Main Mall, British Columbia, Canada V6T 1Z1

Received: November 27, 2002; In Final Form: March 19, 2003

Unusual fluorescence characteristics of a carbocyanine dye/octadecanol layer adsorbed onto a Au(111) electrode surface are described. The potential of the electrochemical interface controls the distance separating a previously adsorbed organic layer and the metal electrode by way of a unique adsorption/desorption process. The behavior of the fluorescent-labeled organic layer was monitored under full potential control with epi-fluorescence microscopy and image analysis. For an adsorbed layer, fluorescence is quenched by nonradiative energy transfer into the metal. When desorbed, intense fluorescence was observed due to the separation of the surfactant from the metal surface. In this desorbed state, the surfactant displayed a strong decay in fluorescence intensity with time (loss of 90% over 20 min). We describe two parallel pathways for this fluorescence decay: irreversible photodestruction of the carbocyanine fluorophore and reversible fluorophore aggregation resulting in a decrease in monomer fluorescence. Readsorption of the surfactant layer onto the metal electrode resulted in a near total (85%) recovery of fluorescence measured after desorption of the surfactant layer. The readsorption of the organic monolayer onto the electrode was believed to convert the nonfluorescent aggregates back to the monomer form. These observations were made possible due to the control of the distance separating the fluorescent-labeled organic layer from the metal afforded by the electrical variable.

1. Introduction

The adsorption of lipid-like surfactants onto electrified interfaces has received attention for application in chemical and biochemical sensors.[1] Many techniques have been employed to characterize these unique interfaces including epi-fluorescence microscopy and elastic light scattering[2−6] experiments. We are involved in the development of new, nondestructive techniques capable of in-situ monitoring the behavior of these surfactants at a charged surface. Present investigations are focused on the characterization of octadecanol adsorbed onto the Au(111)/$KClO_4$ interface. The electrochemical response of octadecanol on Au(111) has been extensively studied, and a mechanism of repeatable adsorption/desorption of the surfactant to/from the metal electrode has been proposed.[6] Octadecanol adsorbs onto the uncharged metal surface (at the potential of zero charge (pzc)) as indicated by a depression in the interfacial capacitance. Charging the electrode negatively increases the interfacial capacitance to values equivalent to a water covered surface signifying desorption of the species from the metal surface. By mixing octadecanol with a small amount of the carbocyanine dye DiIC18(5) (1,1′-dioctadecyl-3,3,3′,3′-tetramethylindodicarbocyanine perchlorate), we recently characterized the structure/morphology of the desorbed species using epi-fluorescence microscopy. Carbocyanine dyes are a class of fluorophores mainly utilized as biomembrane probes since they intercalate well into lipid membranes due to their long alkyl chains.[7−10] Our imaging experiments[2] revealed that the surfactant exists as a heterogeneous structure when desorbed into the aqueous phase and suffers no change in its morphology even after numerous cycles of adsorption/desorption as long as slow potential perturbations are used. Furthermore, the desorbed surfactant was found not to diffuse away from this region near the electrode even after several minutes. Since the surfactant does not diffuse (within the resolution of this technique), it is possible to characterize the photophysics of the dye in an octadecanol matrix at various distances from the metal over long periods of time. Such investigations are related to radiative decay engineering.[11]

Much of the photophysics of dye molecules can be summarized in a simple Jablonski diagram[12] depicting numerous fates for a dye molecule in the excited state. Common fates include relaxation to the ground state via radiative pathways such as fluorescence or phosphorescence. Nonradiative pathways can include quenching of fluorescence or phosphorescence by quencher molecules in solution. Furthermore, the photophysics are strongly dependent on the type of dye and environment in which experiments are conducted. In the investigations described in this report, we are interested in measuring fluorescence emission from a carbocyanine fluorophore in octadecanol near a metal surface. Proximity of fluorophores to metal surfaces can impact fluorescence intensity, quantum yield, and excited-state lifetimes.[13−18] The magnitude of these effects is influenced by the distance separating the fluorophore from the metal. Kuhn and co-workers[13,18] were the first to investigate the absorption/emission of light from a fluorophore near an evaporated silver mirror on a glass substrate. It was found that the excited-state lifetime of the dye varies with separation from the metal. At small separations (<50 nm) the excited-state lifetime approaches zero due to nonradiative energy transfer into the metal. This quenching efficiency diminishes as the fourth power of increasing separation between the metal and fluorophore.[14] In addition to fluorescence quenching, a recent review[11,19] discusses alternate influences of the metal surface on the radiative properties of the dye. Nearby rough thin metal substrates increase the radiative decay rate of low quantum yield chromophores, resulting in an enhancement of fluorescence by

* To whom correspondence should be addressed. E-mail: bizzotto@chem.ubc.ca.

10.1021/jp0275746 CCC: $25.00
Published on Web 07/24/2003

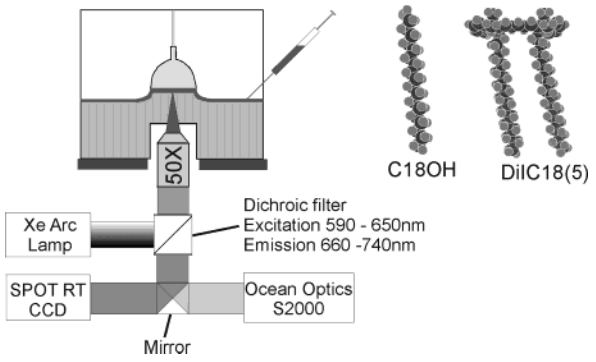

Figure 1. Schematic diagram of the spectroelectrochemical setup used for in-situ fluorescence microscopy. The bottom mirror redirects the filtered emission to the camera or the spectrometer. Space-filling models of octadecanol (C18OH) and DiIC18(5) dye are also shown.

factors up to 1000. These effects were explained as due to the oscillating dipole of the fluorophore interacting with the free electrons in the metal and not attributed to reflection from the mirror surface. The metal surface was also predicted to increase the photostability of the nearby dye.

Cyanine dyes often have another fate associated with their environment as they are known to undergo self-association in the form of aggregates in solution, on the water surface, and on solid surfaces.[20−23] Compared to the monomer absorption and emission, the aggregated complex can give rise to a shifted absorption/emission profile. These aggregates have been referred to as J and H aggregates since their discovery in 1936.[24] Since then, there have been many investigations on the behavior of these aggregates both in solution and on solid phases for their application in photography.[23] Some reports have elucidated the structure or framework of the aggregated complex and its effect on the photophysics of the dye,[25,26] yet the number of monomers that make up an aggregate has not been clearly defined. These aggregated complexes have been shown to be reversible to the monomer form with changes in temperature.[21] We report here on the ability to electrochemically control the distance separating a dye/octadecanol layer from a metal surface and the effects this has on the radiative decay of the dye. We describe a unique observation of fluorescence recovery by the electrosorption process after apparent photobleaching of dye molecules.

2. Experimental

2.1. Electrochemical Method. Electrochemical investigations were carried out in a standard three-electrode cell. The working electrode (Au(111)) was set in a hanging meniscus arrangement with a gold counter electrode and a reference electrode (SCE) connected to the working solution through a salt bridge. The electrolyte was 50 mM $KClO_4$ dissolved in MilliQ water (>18.2 MΩ) and deaerated with Ar (PraxAir, cleaned with a Supelco charcoal filter). Electrochemical characterization of the electrode/electrolyte interface was carried out using standard electrochemical techniques (cyclic voltammetry, differential capacitance). To deposit the surfactant, an aliquot of octadecanol (Sigma) dissolved in chloroform (3 mg/mL) with 3 mol % of DiIC18(5) (Molecular Probes, used as received) was introduced onto the surface of the electrolyte and a monolayer formed after solvent evaporation (Figure 1). The working electrode was flame annealed, allowed to cool in the Ar atmosphere, and under potential control (0 V/SCE) touched to the surface of the electrolyte, thereby transferring the surfactant from the solution surface to the electrode. It was shown previously[2] that the addition of the dye only caused slight disruptions in the electrochemical characterization. The results discussed in this report were obtained with 3 mol % concentrations of the dye in octadecanol.

2.2. Epi-Fluorescent Setup. Fluorescence imaging was conducted with an inverted epi-fluorescent microscope (Olympus IX70) equipped with a 50× objective (NA = 0.5, wd = 10 mm) and a Chroma filter cube (Set 41008, excitation 620 nm (fwhm 60), dichroic 660 nm, emission 700 nm (fwhm75)). The inverted microscopic arrangement enabled looking up onto the metal surface as shown in Figure 1. The objective port in the spectroelectrochemical cell was a coverglass (0.17 mm thick) sealed onto the glass body. All of the images presented were captured with a 50× objective and a SPOT RT digital camera. Each image has a bit depth of 8, resulting in 256 gray levels, and each image also has 2 × 2 binning with an exposure time of 10 s. The above parameters result in a resolution of 0.385 μm/pixel. Fluorescence spectra were measured using an Ocean Optics fiber optic spectrometer coupled to the camera port of the microscope. The wavelengths measured are limited to the band-pass of the filter cube used.

2.3. Epi-Fluorescent Imaging. After electrochemical characterization of a 3 mol % DiIC18(5)/octadecanol layer was accomplished, fluorescence images of the interface were acquired to characterize the decay in fluorescence with time. The fluorescence images were acquired at only two potentials: adsorption potential images (E_{ads} = 0 V/SCE) and desorption potential images (E_{des} = −0.800 V/SCE). Typically, the potential was held for a total of 5 min at E_{ads}, and during this time, fluorescence images of the electrode surface with adsorbed surfactant were recorded at 1 min intervals. The potential was then pulsed to E_{des} for 20 min where, during this time, a series of fluorescence images were recorded at 1 min intervals. We will be reporting the data in terms of decay number where the 5 min at E_{ads} followed by the 20 min at E_{des} will be referred to as 'one decay'. Typically, 5−6 decay experiments were sequentially performed on one adsorbed layer, yielding a series of images, which were analyzed as described next.

2.4. Epi-Fluorescent Image Analysis. All fluorescence images were analyzed using dip_image routines for Matlab.[27] Correction for nonuniform illumination was achieved by acquiring a fluorescence image of the electrode surface prior to introduction of surfactant (I_o). Essentially, this image is of light leaking through the barrier filters and represents the spatial distribution of the intensity of the incident light. After smoothing, the image was used to correct for the spatial variation in intensity by dividing through each subsequent image collected. These images then represent fluorescence intensity normalized for the variation in the incident radiation (I/I_o). For each decay (5 min at E_{ads} and 20 min at E_{des}) the I/I_o adsorption images were averaged together to correct for the nonblack background. The resulting average image was then subtracted from every image in the corresponding decay, yielding images that represent normalized differences in fluorescence intensity ($\Delta I/I_o$). This was repeated for all decays, and all average intensity measurements were based upon these normalized difference images. The $\Delta I/I_o$ images were then segmented so that only regions of moderate fluorescence intensity were analyzed, ensuring that the analysis occurred only for regions that give rise to a substantial change in the fluorescence. In this way, the resulting analysis would not be biased by regions that were not highly fluorescent. In some cases, small regions of very intense fluorescence were also observed. These regions were also excluded from the analysis by a masking routine since the CCD response may not be linear with photon flux at these saturation

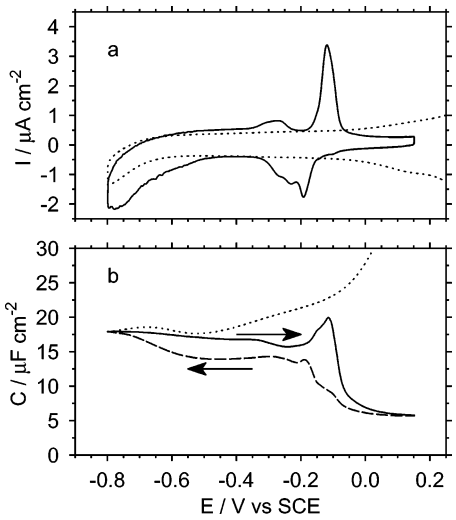

Figure 2. (a) Cyclic voltammetry (20 mV/s) and (b) differential capacitance (5 mV/s, 5mV rms, 25 Hz) measurements of Au(111) in contact with 50 mM $KClO_4$ (dotted line) and in contact with 3 mol % DiIC18(5)/octadecanol monolayer (solid and dashed lines, arrows indicate direction of potential scan).

levels. As a safeguard, the mask was significantly expanded via a number of dilation steps to exclude all intense features throughout the experiment. This mask was then applied to every $\Delta I/I_o$ image in the experiment, thereby excluding the intense features. Histograms for each of the masked $\Delta I/I_o$ images were calculated. The average fluorescence intensity for each masked image was considered proportional to the average of the histogram.

3. Results

3.1. Electrochemical Characterization. The adsorbed layer of 3 mol % DiIC18(5)/octadecanol was characterized with cyclic voltammetry (CV) and differential capacitance measurements prior to the spectroelectrochemical investigations. A detailed discussion of the electrochemical characterization is described in ref 28. Briefly, Figure 2a represents the CV of Au(111) in contact with $KClO_4$ (dotted line) and adsorbed surfactant (solid line). Au(111) in contact with the supporting electrolyte is ideally polarizable in the potential range of interest (0.200 to −0.800V/SCE). In the presence of an adsorbed surfactant layer, peaks are observed which correspond to changes in the interfacial capacitance due to potential-driven phase changes in the adsorbed surfactant layer. Since the interface can be simply modeled as a capacitor in this potential window, a more quantitative discussion will center around the differential capacitance measurements shown in Figure 2b. At positive potentials, the presence of adsorbed surfactant lowers the capacitance to a value of roughly 5−6 μF cm^{-2}. Scanning the potential negatively, the capacitance remains depressed but slowly rises to a value slightly above 10 μF cm^{-2} in the region from −0.150 to −0.300 V/SCE. Scanning the potential even further negative, the interfacial capacitance continues to increase until it reaches a value for a water-covered surface (17 μF cm^{-2}) signifying desorption. On the positive going return scan, the capacitance remains high, exhibiting significant hysteresis due to the difference in the adsorption and desorption processes. A peak in the capacitance due to the readsorption of the surfactant layer was observed at −0.125 V/SCE, followed by a significant lowering of capacitance and reestablishment of the adsorbed surfactant layer. The results shown in Figure 2 represent one scan from numerous repeatable adsorption/desorption cycles.

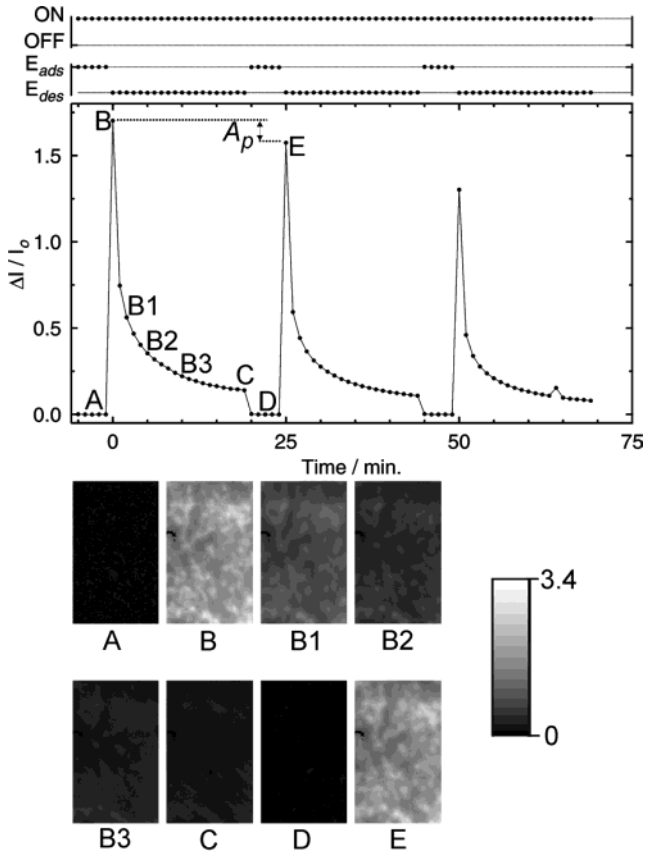

Figure 3. Fluorescence intensities calculated for three consecutive decays collected from the same region on the electrode and the same surfactant layer under continuous illumination. Images A−E (95 × 140 μm) correspond to the times indicated on the first decay trend. The calculation of A_p for the initial decay is shown.

These results with the accompanying fluorescence images have been described in more detail.[2] We believe that interfacial potential exerts control, through interfacial tension, over the separation between the metal and surfactant. This control allowed for potential modulation of the fluorescence yield and has led to an unusual observation of fluorescence recovery due to electrosorption, which is described below.

3.2. Fluorescence Decays and Recoveries Under Constant Illumination. A series of fluorescence images were collected for six consecutive decays (six cycles of 5 min at E_{ads} followed by 20 min at E_{des}) with the first three decays shown in Figure 3. In this experiment five images were collected at E_{ads} and 20 images collected at E_{des}, repeated 6 times yielding 150 images all acquired from the same region of the electrode, under constant illumination and with the same acquisition conditions. The average gray scale of the first adsorption images are zero due to the reduction in fluorescence lifetime because of the fluorophore's proximity to the electrode surface, quenching the fluorescence. This is shown in image A. The first desorption potential (E_{des}) image for the first decay (image B) had an average gray scale of 1.75. The intensity of the fluorescence images taken during 20 min at E_{des} clearly illustrates a profound decrease (images labeled B1, B2, B3). In fact, the last image recorded at E_{des} (image C) is quite weak. The second decay is initiated by readsorption of the surfactant. The fluorescent images are dark due to the quenching of the fluorescence as shown in both the average gray scale values and image D. The first image at E_{des} in the second decay resulted in a surprisingly strong fluorescence image E. This apparent recovery of the fluorescence gives images that are close in intensity to the

original desorption potential image (B) and represents a recovery of 92.5%. Repeating the potential perturbations and measuring the resulting fluorescence images shows that this recovery process can be sustained with recovery efficiencies (compared to the previous decay's first E_{des} image) of 83%, 81%, 87%, and 86% (data for the last three decays not shown). This series of experiments clearly illustrates the link between fluorescence recovery and the changes in potential which effectively manipulates the separation between the electrode and the desorbed surfactant. Clearly, the recovery by electrosorption is not total, suggesting that fluorescence will continually decrease to an undetectable level with repeated investigations on the same layer. This fluorescence recovery was reproducibly achieved, and although the magnitude of the fluorescence image intensities were variable, the degree of the fluorescence recoveries were always >80%.

4. Discussion

The observed recovery of fluorescence intensity with changes in potential, or more strictly changes in separation of the dye from the metal, was unexpected. A number of possible explanations for this phenomena can be imagined, and we shall deal with each in turn in the following discussion.

4.1. Fluorescence Recovery After Photobleaching (FRAP). The observation of a fluorescence recovery is usually associated with FRAP.[29] In FRAP, a small section in the field of view is exposed to an intense pulse of radiation, photobleaching the dye molecules and rendering a small region (micrometer sized) fluorescently dark. Recovery of the fluorescence in this small region is governed by the lateral diffusion of the surrounding dye molecules into the dark region at a rate controlled by diffusion. This method is typically used to measure the diffusion coefficient of dye within lipid monolayers. Although our system does not involve an intense pulse of radiation, photobleaching may still occur due to the extent of illumination time (20 min). The images collected, however, clearly illustrate the lack of diffusion or change in structure/morphology of the desorbed surfactant layer, even after a number of adsorption/desorption cycles. The diffusion of 'new' fluorophore into the region is unlikely since the diffusion lengths needed would be quite large (0.1 mm). Another explanation for fluorescence recovery in our system is required.

4.2. Influence of Light Exposure Time. Extended illumination will continually promote ground-state fluorophores to an excited state where a number of nonfluorescent fates exist for the dye molecules. A molecule in the singlet excited state can move to a triplet state by way of intersystem crossing. Triplet states are long-lived in comparison to singlet states and can result in phosphorescence. This could be a possibility for the observed decay under constant illumination. The observed recovery upon readsorption may be due to these triplet states relaxing to the ground state by energy transfer to the metal. Another possible fate for an excited-state molecule is to form a complex with a neighboring ground-state molecule, forming an exciplex. The exciplex may be nonfluorescent, or fluoresce at strongly red-shifted frequencies, beyond our filter set. Readsorption of the surfactant may disrupt the exciplex, yielding monomers able to participate again in fluorescence when desorbed. In both scenarios, the decay depends on the extent of illumination. A decrease in illumination time should drastically affect the fluorescence decay. Typically, triplet states for carbocyanine dyes decay in milliseconds,[30−32] so blocking the light source should allow the desorbed molecules in the triplet state to relax to the ground state via phosphorescence and allow for a fluorescence recovery without changes in electrode potential. Furthermore, the extended time without illumination would decrease the concentration of the excited state enormously, effectively eliminating the possibility of exciplex formation.

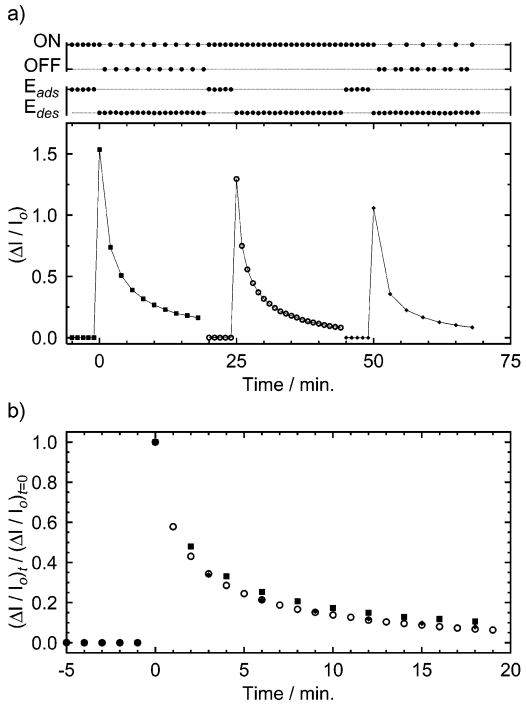

Figure 4. Fluorescence decay profiles measured under intermittent (■,◆) and constant (○) light exposure (see text for details): (a) Fluorescence decay transients and (b) decay transients normalized to the first E_{des} image in the decay.

These possibilities were tested by blocking the excitation light for various lengths of time, during the monitoring of fluorescence decay. Figure 4a shows the results of three decays for which the excitation source was manually blocked for various intervals over the 20 min spent at the desorption potential. All images collected at E_{ads} were acquired during uninterrupted illumination. The first decay was performed with the light alternating between on and off at 1 min intervals (1 min on/1 min off), resulting in 10 fluorescence images over 20 min at E_{des}. The second decay was acquired as in Figure 3 with constant illumination, giving 20 fluorescence images. The third decay was collected with the light alternating between 1 min on and 2 min off, yielding six fluorescence images during the 20 min spent at E_{des}.

When comparing the data collected under intermittent light conditions (Figure 4a) to the data collected under constant illumination conditions, no clear differences were observed. Clearly, the length of exposure to excitation is not an important factor in both the decay and recovery. This is further emphasized in Figure 4b, where the three decays are compared by normalization to the average intensity of the first desorption image in each decay. No apparent difference in the decay profiles was noticed between the decays where excitation was continuously on (○) and where excitation was intermittent. It is clear the triplet state or exiplex formation is not causing the decay trends observed. Also evident from this investigation is that a fluorescence decay pathway exists which is light independent. However, we again observed a lack of 100% recovery, indicating an irreversible loss of fluorophore must also occur, suggesting at least two possible parallel processes.

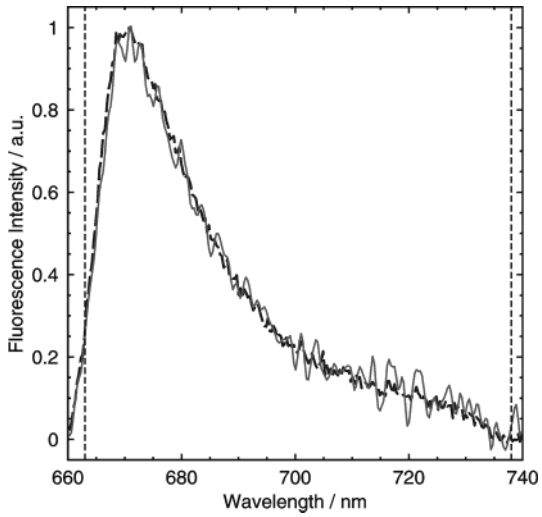

Figure 5. Normalized fluorescence spectra of the desorbed surfactant layer acquired for a freshly desorbed layer (dashed line) and for the same desorbed layer after 20 min of constant exposure to light (solid line). The spectra are limited by the band-pass of the emission filter set used.

4.3. Radiative Enhancement. The presence of a metal surface may provide other alternative explanations for the observed recovery. According to recent literature, for certain separations between the surfactant and the metal, a significant enhancement of fluorescence may be observed.[33,34] This enhancement region is believed to exist for separations on the order of nanometers. Thus, it is possible that upon desorption, the surfactant is present in this region of enhancement, which then drifts out of this special region with time. We believe that this possibility is unlikely in our system because of the nature of the metal used. The literature on the subject of fluorescence enhancement due to a metal surface is closely related to SERS effect, where the enhancement is most efficient due to the coupling of light with surface plasmons on very rough surfaces.[35] The description of fluorescence enhancement seems to be a popular topic with silver island thin films where the surfaces are rough[33,36] and the enhancement is particularly evident for low quantum yield fluorophores.[19] We believe that the smooth surface of Au(111) in our experiments coupled with the high quantum yield of DiIC18(5) dye used eliminates this possibility. Though not definitive, future work will not ignore this aspect.

4.4. Light-Independent Dye Aggregation. Carbocyanine dye molecules self-aggregate, a process which is reversible with temperature and specific to the aggregate environment.[20−23] These aggregated dye complexes have a significant effect on the spectral properties of the dye. Compared to the monomer, an aggregated complex can induce shifts in the absorption/emission profile,[20] red-shifted fluorescence (J-aggregate) or a blue-shifted absorption (H-aggregate), or result in the creation of a nonfluorescent complex. Investigations on DiIC18(5) have been conducted on the water and glass surface.[22] Aggregation of DiIC18(5) occurred more readily on the water surface because of the less restricted microenvironment. These results suggest that the light-independent pathway dominant in the observed decays may be the result of formation of an aggregated complex of carbocyanine dye. This aggregated complex will significantly change the photophysics of the dye, possibly altering the fluorescence emission profile to wavelengths outside our observation window. Measurement of the fluorescence spectrum during the decay experiments is shown in Figure 5. The spectra were acquired with the imaging filters in place, and so only a restricted wavelength range could be examined. An emission spectrum measured after 1 min at E_{des} followed by an emission spectrum measured after 20 min at E_{des} are compared in Figure 5. No change in the fluorescence emission profile over 20 min was evident, suggesting that any shift in fluorescence emission wavelength must be considerably larger than 60 nm.

A more likely possibility is that the absorption spectrum for the aggregated species lies outside of our excitation wavelength range. Aggregation then 'protects' the dye from photobleaching but reduces fluorescence since the complex is no longer absorbing photons. Alternatively, the new aggregate may not fluoresce at all. In both scenarios, the decrease in fluorescence occurs because fluorescence can only be generated from the monomer form of the dye, which decreases with time at the desorption potential due to aggregation. Readsorption onto the metal surface reverts the aggregate to its monomer form, ready to fluoresce once re-desorbed. This explanation is clearly supported by the experimental evidence as well as the modeling discussed next.

5. Proposed Model

The collected experimental evidence suggests that at least two pathways are responsible for the fate of the dye molecules in the desorbed surfactant layer. One path is dependent on exposure to excitation light and induces irreversible changes to the fluorescence intensity. The other pathway is light independent and causes changes that are reversible once the surfactant layer is readsorbed onto the metal.

Experimentally, we can only measure the fluorescence intensity ($\Delta I/I_o$) which is assumed to be proportional to concentration of monomer dye molecules. Since the separation between the fluorophore and metal strongly influences the radiative lifetime, the model must assume a minimum value for this distance. The quenching of fluorescence due to the presence of a metal surface is nonlinearly dependent on the separation between the metal and surfactant containing dye layer. Therefore, the model assumes that this layer exists far enough away from the metal such that even partial quenching does not occur. Therefore, our model only applies at the desorption potential and presupposes the separation between the surfactant from the metal (see Figure 8). Furthermore, we will treat each of the consecutive decays such that time is reset to zero for the first desorption potential image in each decay. A ground-state molecule of the carbocyanine dye (A) can undergo three principal reactions: (1) A can absorb a photon, move to the first excited state, and then relax to the ground-state, emitting a photon at the fluorescence wavelength; (2) A can absorb a photon and irreversibly photodecompose with a rate constant k_p, resulting in a new compound(s) (A_P) that is(are) no longer fluorescent and therefore unobservable by our experiment; or (3) two ground-state molecules of dye could form an aggregated complex (J) with a rate constant k_a, inducing a shift in the absorption band (or nonfluorescent complex) out of the excitation wavelength range, thereby reducing the observed fluorescence. The formation of J is reversed upon readsorption onto the metal surface, creating monomers that can again participate in the fluorescence. Of these three possibilities, the first can be ignored in the model since the excited-state lifetime of a fluorescence event is short when compared to the other two processes. The remaining two parallel processes can be described by

$$A + h\nu \xrightarrow{k_p} A_p$$

$$A + A \xrightarrow{k_a} J \qquad (1)$$

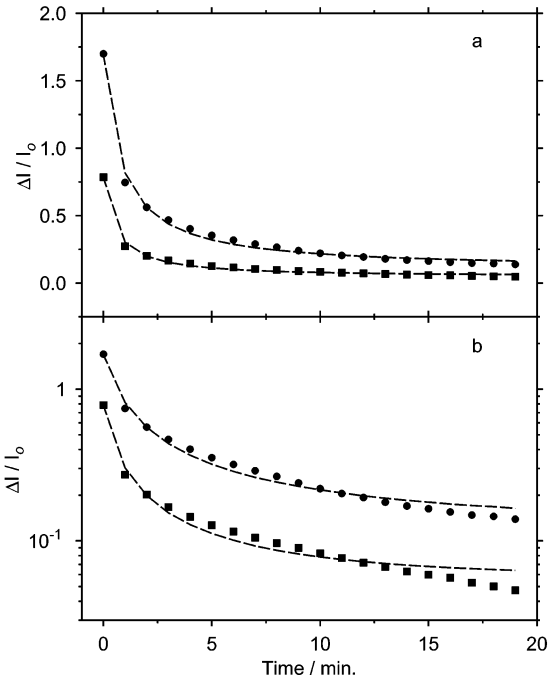

Figure 6. Experimental (first ● and sixth ■ decay taken from Figure 3) and model (line) fluorescence decays: (a) linear plot and (b) logarithmic plot.

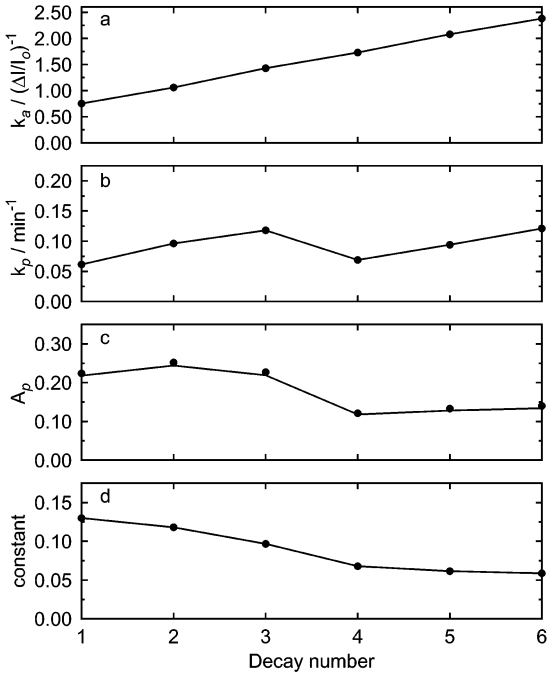

Figure 7. Parameters from fitting the data in Figure 3 to the proposed model: (a) aggregation rate constant, k_a, (b) photodecomposition rate constant, k_p, (c) amount of photodecomposed A, A_p, and (d) scattered light contribution modelled as a time-independent constant.

We use fluorescence intensity as a measure of the concentration of free unassociated monomer dye molecules (A), remembering that only frequencies of light emitted within our band-pass wavelength range was observed. With a constant flux of photons (guaranteed through our normalization correction), the change in A with time can be written as

$$\frac{d[A]}{dt} = -k_p[A] - k_a[A]^2 \qquad (2)$$

Integration of the above equation, using the intensity of the first desorption image for each decay (A_o) as an integration limit ($t = 0$), yields the temporal evolution of A

$$A(t) = \frac{k_p A_o \exp(-k_p t)}{(k_p + A_o k_a - k_a A_o \exp(-k_p t))} \qquad (3)$$

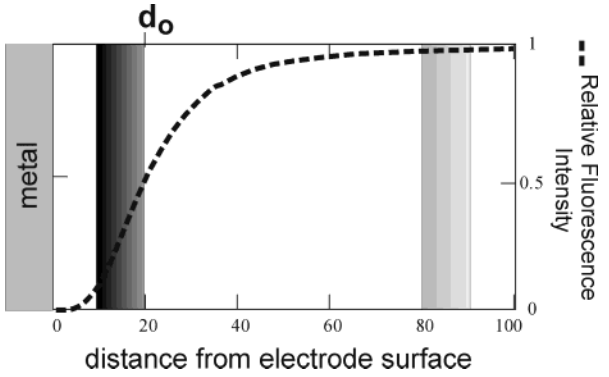

Figure 8. Schematic depiction of the fluorescence quenching profile and the position of the desorbed organic layer, shown as a slab. The intensity of the fluorescence is represented by an increase in the gray scale of the slab. The model initially proposed assumes that the desorbed surfactant layer exists as the slab that is furthest from the electrode. Further analysis of the modeling results suggests the surfactant slab is much closer to the electrode. d_o is the characteristic length for the fluorescence quenching profile.

The changes in fluorescence intensity with time are fit to this general equation along with one additional piece of data. From experiment, the amount of photodecomposed dye can be determined by calculating the difference between two consecutively desorbed layers just after the potential step from E_{ads}. For example, the difference between point B and E in Figure 3 is assumed to be the amount of photobleached product irreversibly formed. The amount of A_p at any time after the desorption of the surfactant layer can be determined from integration of $(d[A_p]/dt)] = k_p[A]$ to give

$$A_p(t) = \frac{k_p}{k_a} \log\left\{\frac{(k_p + A_o k_a - k_a A_o \exp(-k_p t))}{k_p}\right\} \qquad (4)$$

The decays measured are 20 min long, so based upon the parameters used in the model, the amount of photobleached A can be calculated and compared to the observed loss in fluorescence intensity.

Fitting of the model to each individual experimental decay was performed using the data shown in Figure 3. A least-squares fitting based upon a Matlab optimization routine (Nedler−Mead simplex method) was used. Equation 3 was modified by addition of a constant term, which was required because of the increase in background due to elastically scattered light. Since fluorescence intensity is used as a measure of [A], any difference in the background between the E_{des} and E_{ads} images will be present as an unchanging offset. Previous studies on this system showed that scattering of light was significantly larger at the desorption potential when compared to the adsorption potential.[3] Since $\Delta I/I_o$ is the measured parameter, additional contribution from the scattered light present in the desorbed images will result in an offset that is not accounted for in our kinetic model. The scattered light is strongly attenuated by the filter set used, but a small amount of leakage can be expected. The fit of a modified eq 3 to the data resulted in values for both rate constants, k_a and k_p as well as the constant with regression coefficients of >0.997.

The experimental data (symbols) and the resulting model fit (lines) are shown in Figure 6. Figure 6a represents the experimental and fit results from the first (●) and sixth (■) decays from the data in Figure 3 (sixth decay not shown). For comparison, Figure 6b represents the same experimental and fitted results plotted on a logarithmic scale, illustrating the deviation from exponential decay. The model fits the experimental data very well with the inclusion of the constant parameter. The resulting fit parameters are shown in Figure 7 as a function of the decay number. Many other data sets have been analyzed in the same manner, giving the same trends, although the absolute numbers for the rate constants depend on the characteristics of the image under analysis. The rate constants, the constant offset, and the amount of photodecomposed A (A_p) are all compared. Generally, k_a is an order of magnitude larger than k_p and also increases with decay number, while k_p remains essentially constant. The offset is small and slowly decreases with decay number. A_p also decreases with decay number.

The relative magnitudes of the rate constants indicate that the reversible aggregation process dominates and a small amount of irreversible photobleaching occurs. The aggregation effectively protects the dye from photobleaching, resulting in a small amount of photobleached dye and larger recoveries of the fluorescence after adsorption/desorption. The decrease in A_p is expected since exposure of the desorbed layer to light increases with decay number. As the layer is repeatedly exposed to light, photobleaching removes some of the fluorescing A molecules (those furthest from the electrode first since their lifetimes are much longer). This process results in a decrease in the rate of photodecomposition and, hence, a decrease in A_p with decay number, though k_p remains constant.

The slight decrease in the constant results from the change in the efficiency of the scattering of light from the surfactant aggregates. We have shown[3] through elastic light scattering and fluorescence imaging measurements that the desorbed layer does subtlety change with repeated adsorption/desorption cycles, and so a small change in the scattered light can be expected. It should be emphasized that this constant is a small component of the overall measured signal.

The increase in k_a by over a factor of 3 with decay number is surprising and reflects that our system is more complex than the simple model proposed. Inherent in our model was the assumption that fluorescence intensity is a measure of all A in our system, and therefore, all dye must exist far enough from the metal such that quenching is not important. This assumption cannot be correct. Figure 8 illustrates a simplified depiction of our system with the organic film shown as a slab. The relative fluorescence intensity profile is also shown, taking into account the quenching effect of the metal, with its characteristic length d_o where 50% of the fluorescence is quenched. In our model, at the desorption potential, the surfactant layer was assumed to exist in a region where quenching does not occur (at a separation much greater than d_o). If the surfactant layer exists closer to the electrode surface, a certain population of A, called A_q, will not fluoresce and their existence will not be recognized in our model. This population of dye molecules could still form aggregates between themselves, A_q-A_q, or with a fluorescing partner, A_q–A. This possibility explains the increase in k_a with decay number. The rate of aggregation is now no longer simply measured by eq 1 since the fluorescence intensity is no longer an accurate measure of the total concentration of A ($= [A] + [A_q]$) but only of the fluorescing monomer species [A]. The real rate of aggregation with rate constant k'_a is given by

$$\text{rate of aggregation} = k'_a[A + A_q]^2 = k'_a([A]^2 + [A_q][A] + [A_q]^2) \quad (5)$$

The model assumes an aggregation rate of $k_a\,[A]^2$. It is clear that the model rate constant actually represents

$$k_a = k'_a\left(1 + \frac{[A_q]}{[A]} + \frac{[A_q]^2}{[A]^2}\right) \quad (6)$$

With increasing exposure to light, the amount of fluorescing A, [A] decreases while the amount of nonfluorescing A, [A_q] remains constant. This effect is manifested as an increasing k_a with decay number since A_q can participate in the aggregation process as an invisible partner.

For the system described, the existence of these aggregates was shown only indirectly. Direct proof of the existence of these aggregates in the desorbed monolayer will require the measurement of the changes in the absorption spectrum of the desorbed molecules over time. We suspect that the aggregation of the dye molecules will form a complex which does not absorb the narrow band of radiation available in our experimental setup. We will use electroreflectance spectroscopy to measure the difference in the absorption spectra between the adsorbed and desorbed state (both at 0 and 20 min). These measurements will indicate if the observed fluorescence decay and recovery was due to nonfluorescent aggregates or to a blue shift in the absorption spectrum. Further studies on characterization of the distance dependence of the fluorescence intensity and lifetimes are also underway. These final experiments will identify the origin of the unusual fluorescence recovery results presented.

6. Conclusions

The fluorescence behavior of electrochemically desorbed aggregates of water-insoluble surfactants (containing a small amount of a fluorescent dye) was described. An unusual recovery of fluorescence intensity controlled electrochemically was presented and a model explaining this behavior proposed. A strongly decreasing fluorescence signal with time was observed for the surfactant layer when desorbed off the electrode surface. The fluorescence intensity surprisingly recovered to >80% of its original values by simply cycling the potential through an adsorption/desorption process. This fluorescence decay was dominated by aggregation of the dye (a process independent of exposure to light), forming a complex which we believe does not absorb light under the conditions of the experiment, effectively reducing fluorescence intensity. Fluorescence recovery was attributed to the readsorption process which reverted the complex back to the monomer form, allowing for the increase in fluorescence intensity. The dye also suffers from photobleaching, and the proposed model develops these two parallel pathways: photobleaching and aggregate formation which explain the results observed quite well. The aggregation rate constant is ~10−40× greater than the rate constant for the photodecomposition process. Analysis of consecutive decays revealed that the desorbed surfactant must exist near the electrode in a region that experiences fluorescence quenching effects. Overall, these results demonstrate the possibility for electrochemical control of radiative characteristics of a fluorophore. This control stems from the ability of electrochemical techniques to manipulate the interfacial tension of the metal/solution interface, which controls the distance/separation between the metal surface and the desorbed surfactant layer.

Acknowledgment. The authors are grateful to NSERC for operating and equipment funding. J.S. is supported through a PGS from NSERC. Support from Imperial Oil University Research Grant is also gratefully acknowledged. The authors express their thanks to B. Ditchburn for his efforts in glassblowing our spectroelectrochemical cell.

References and Notes

(1) Swalen, J.; Allara, D.; Andrade, D.; Chandross, E. A.; Garoff, S.; Israelachvili, J.; McCarthy, T. J.; Murray, R.; Pease, R. F.; Rabolt, J. F.; Wynne, K. J.; Yu, H. *Langmuir* **1987**, *3*, 932−950.

(2) Shepherd, J.; Yang, Y.; Bizzotto, D. *J. Electroanal. Chem.* **2002**, *524*−*525*, 54−61.

(3) Yang, Y. G.; Bizzotto, D. *J. Electroanal. Chem.* **2001**, *500* (1−2 Special Issue SI), 408−417.

(4) Bizzotto, D.; Wong, E.; Yang, Y. G. *J. Electroanal. Chem.* **2000**, *480* (1−2), 233−240.

(5) Bizzotto, D.; Pettinger, B. *Langmuir* **1999**, *15* (23), 8309−8314.

(6) Bizzotto, D.; Zamlynny, V.; Burgess, I.; Jeffrey, C. A.; Li, H.-Q.; Rubinstein, J.; Galus, Z.; Nelson, A.; Pettinger, B.; Merril, R. A.; Lipkowski, J. In *Interfacial Electrochemistry*; Wieckowski, A., Ed.; M Dekker: New York, 1999; pp 405−426.

(7) Krasne, S. *Biophys. J.* **1980**, *30* (3), 415−439.

(8) Krasne, S. *Biophys. J.* **1980**, *30* (3), 441−462.

(9) Sims, P. J.; Waggoner, A. S.; Wang, C.-H.; Hoffman, J. F. *Biochemistry* **1974**, *13* (16), 3315−3330.

(10) Wolf, D. E. In *Spectroscopic Membrane Probes*; Loew, L. M., Ed.; CRC Press: Boca Raton, FL, 1988; Vol. 1, pp 240.

(11) Lakowicz, J. R.; Shen, Y.; D'Auria, S.; Malicka, J.; Fang, J.; Gryczynski, Z.; Gryczynski, I. *Anal. Biochem.* **2002**, *301* (2), 261−277.

(12) *Principals of Fluorescence Spectroscopy*; Lakowicz, J. R., Ed.; Plenum Press: New York, 1983.

(13) Kuhn, H.; Möbius, D.; Bücher, H. In *Physical Methods of Chemistry. Part IIIB Optical, Spectroscopic, and Radioactivity Methods*; Weissberger, A., Rossiter, B. W., Eds.; Wiley-Interscience: New York, 1972; Vol. 1, pp 577−578.

(14) Chance, R. R.; Prock, A.; Silbey, R. In *Advances in Chemical Physics*; Prigogine, I., Ed.; Interscience Publishers: New York, 1978; Vol. 37, pp 1−65.

(15) Drexhage, K. H.; Kuhn, H.; Schafer, F. P. *Ber. Bunsen-Ges. Phys. Chem.* **1968**, *72*, 329.

(16) Drexhage, K. H. *J. Lumin.* **1970**, *1/2*, 693.

(17) Drexhage, K. H. In *Progress in Optics*; Wolf, E., Ed.; Interscience: Amsterdam, 1974; Vol. 12, pp 163−232.

(18) Kuhn, H.; Moebius, D. In *Physical Methods of Chemistry*, 2nd ed.; Rossiter, B. W., Baetzold, R. C., Eds.; Wiley-Interscience: New York, 1993; Vol. IXB, pp 375−542.

(19) Lakowicz, J. R. *Anal. Biochem.* **2001**, *298* (1), 1−24.

(20) Moebius, D. *Adv. Mater. (Weinheim, Germany)* **1995**, *7* (5), 437−444.

(21) Khairutdinov, R. F.; Serpone, N. *J. Phys. Chem. B* **1997**, *101* (14), 2602−2610.

(22) Slyadnev, M. N.; Inoue, T.; Harata, A.; Ogawa, T. *Colloids Surf., A* **2000**, *164* (2−3), 155−162.

(23) Muenter, A. A.; Brumbaugh, D. V.; Apolito, J.; Horn, L. A.; Spano, F. C.; Mukamel, S. *J. Phys. Chem.* **1992**, *96* (7), 2783−2790.

(24) Jelley, E. E. *Nature* **1936**, *138*, 1009−1010.

(25) von Berlepsch, H.; Boettcher, C.; Ouart, A.; Burger, C.; Daehne, S.; Kirstein, S. *J. Phys. Chem.* . **2000**, *104* (22), 5255−5262.

(26) Czikkely, V.; Foersterling, H. D.; Kuhn, H. *Chem. Phys. Lett.* **1970**, *6* (3), 207−210.

(27) van Vliet, L. J. DIPLib, the Delft Image Processing Library; http://www.ph.tn.tudelft.nl/DIPLib/DIPLib.html.

(28) Bizzotto, D.; Lipkowski, J. *J. Electroanal. Chem.* **1996**, *409* (1−2), 33−43.

(29) Meyvis, T. K. L.; De Smedt, S. C.; Van Oostveldt, P.; Demeester, J. *Pharm. Res.* **1999**, *16* (8), 1153−1162.

(30) Tinnefeld, P.; Herten, D.-P.; Sauer, M. *J. Phys. Chem. A* **2001**, *105* (34), 7989−8003.

(31) Tinnefeld, P.; Buschmann, V.; Herten, D.-P.; Han, K.-T.; Sauer, M. *Single Molecules* **2000**, *1* (3), 215−223.

(32) Cooper, W.; Liebert, N. B. *Photogr. Sci. Eng.* **1972**, *16* (1), 25−34.

(33) Gryczynski, I.; Malicka, J.; Gryczynski, Z.; Geddes, C. D.; Lakowicz, J. R. *J. Fluoresc.* **2002**, *12* (1), 11−13.

(34) Malicka, J.; Gryczynski, I.; Kusba, J.; Shen, Y.; Lakowicz, J. R. *Biochem. Biophys. Res. Commun.* **2002**, *294* (4), 886−892.

(35) Weitz, D. A.; Garoff, S.; Hanson, C. D.; Gramila, T. J.; Gersten, J. I. *J. Lumin.* **1981**, *24*−*25* (1), 83−86.

(36) Leitner, A.; Lippitsch, M. E.; Draxler, S.; Riegler, M.; Aussenegg, F. R. *Appl. Phys. B* **1985**, *36* (2), 105−109.